

## Trapping Alkaline Earth Rydberg Atoms Optical Tweezer Arrays

J. T. Wilson,<sup>1</sup> S. Saskin,<sup>1,2</sup> Y. Meng,<sup>3</sup> S. Ma,<sup>1,2</sup> R. Dilip<sup>Ⓞ</sup>,<sup>2</sup> A. P. Burgers,<sup>1</sup> and J. D. Thompson<sup>Ⓞ</sup><sup>1,\*</sup>

<sup>1</sup>*Department of Electrical Engineering, Princeton University, Princeton, New Jersey 08540, USA*

<sup>2</sup>*Department of Physics, Princeton University, Princeton, New Jersey 08540, USA*

<sup>3</sup>*Vienna Center for Quantum Science and Technology, TU Wien, Atominstitut, Stadionallee 2, 1020 Vienna, Austria*

 (Received 19 December 2019; revised 16 November 2021; accepted 3 January 2022; published 20 January 2022)

Neutral atom qubits with Rydberg-mediated interactions are a leading platform for developing large-scale coherent quantum systems. In the majority of experiments to date, the Rydberg states are not trapped by the same potential that confines ground state atoms, resulting in atom loss and constraints on the achievable interaction time. In this Letter, we demonstrate that the Rydberg states of an alkaline earth atom, ytterbium, can be stably trapped by the same red-detuned optical tweezer that also confines the ground state, by leveraging the polarizability of the  $\text{Yb}^+$  ion core. Using the previously unobserved  $^3S_1$  series, we demonstrate trapped Rydberg atom lifetimes exceeding  $100 \mu\text{s}$ , and observe no evidence of auto- or photoionization from the trap light for these states. We measure a coherence time of  $T_2 = 59 \mu\text{s}$  between two Rydberg levels, exceeding the  $28 \mu\text{s}$  lifetime of untrapped Rydberg atoms under the same conditions. These results are promising for extending the interaction time of Rydberg atom arrays for quantum simulation and computing, and are vital to capitalize on the extended Rydberg lifetimes in circular states or cryogenic environments.

DOI: [10.1103/PhysRevLett.128.033201](https://doi.org/10.1103/PhysRevLett.128.033201)

Arrays of individually trapped neutral atoms with strong interactions via Rydberg excitations are a promising platform for quantum simulation, optimization, and computing [1,2]. The combination of a flexible geometry and highly controllable interactions has enabled explorations of many-body quantum dynamics [3–5], high-fidelity gates [6–11], and the generation of large entangled states [12]. The majority of existing work uses alkali atoms, but recent experiments with alkaline earth atoms in optical tweezers [13–16] suggest a number of technical advantages as well as the potential to apply entangled states to enhance optical atomic clock performance [17,18].

A central challenge to experiments with Rydberg atoms in standard, red-detuned optical tweezers is that the Rydberg states are antitrapped, which gives rise to a repulsive force and a strong light shift. This repulsion arises from the ponderomotive potential of the essentially free Rydberg electron, described by the polarizability  $\alpha_p = -e^2/m_e\omega^2$ , which is always negative [19] (here,  $\omega$  denotes the frequency of the trap light, and  $e, m_e$  are the electron charge and mass). To mitigate this effect, the vast majority of experiments operate with the tweezers turned off during the Rydberg excitation, which limits the interaction time to 10–20  $\mu\text{s}$  because of the expansion of the atoms at typical temperatures of 10 – 20  $\mu\text{K}$ . This is significantly below the typical room temperature Rydberg state lifetime of 100–300  $\mu\text{s}$  for  $n = 60$ –100  $S$  states [2,20], and far below the tens of seconds achievable with circular states in cryogenic cavities [21,22]. Furthermore, heating associated with modulating the trap may impact the gate fidelity in sequential operations.

In recent work, it has been demonstrated that the ponderomotive potential can be used to trap Rydberg atoms in a 3D intensity minimum. Rubidium Rydberg states have been trapped for up to 200  $\mu\text{s}$  in a hollow “bottle beam” generated by a spatial light modulator [23], while simultaneous trapping of ground and Rydberg states has been achieved in a lattice of blue-detuned light sheets, with 50  $\mu\text{s}$  dwell time for atoms in Rydberg states [11]. The stability of these traps requires that the spatial extent of the intensity minimum is large compared to the Rydberg electron orbit ( $R_e = 3n^2a_0/2 \approx 0.8 \mu\text{m}$  for  $n = 100$ ). This necessitates a large-waist optical trap, a corresponding increase in total optical power per trap, and imposes a maximum principal quantum number that can be trapped for a given power, of order  $n = 90$  in Ref. [23]. Ensembles of Rydberg atoms have also been trapped using several approaches [24–28].

In this Letter, we demonstrate an alternate approach: leveraging the polarizability of the  $\text{Yb}^+$  ion core to directly trap Yb Rydberg atoms in conventional, red-detuned optical tweezers [29,30]. Unlike alkali atoms, the ion core of alkaline earth atom Rydberg states has significant polarizability at typical laser trapping wavelengths. The ponderomotive potential of the Rydberg electron contributes an antitrapping effect, but it is small for short wavelengths and high- $n$  Rydberg states where the beam waist is comparable to or smaller than  $R_e$ . We demonstrate trap lifetimes exceeding 100  $\mu\text{s}$  for  $n = 75$  with less than 10 mW of optical power per trap. Trap-induced losses from photoionization are negligible for  $S$  states, but slightly shorten the lifetime of  $P$  and  $D$  states. We study the

interplay of the ponderomotive and  $\text{Yb}^+$  core potentials in detail, including the dependence on the Rydberg level, and observe that “magic” trapping is possible for certain pairs of Rydberg states. A theoretical model is presented to efficiently calculate the trapping potentials by decomposing the potential of the optical tweezer into irreducible tensor operators. We study the coherence properties of a superposition of trapped Rydberg levels, achieving  $T_2 = 59 \mu\text{s}$ , limited by finite temperature and the differential light shift of the two states in the trap but exceeding the lifetime of the Rydberg atom in the absence of the trap. This Letter also presents the first measurement of the lifetime of high- $n$  Yb Rydberg states and the first observation of the  $^3S_1$  Yb Rydberg series.

The trapping potential for Ytterbium Rydberg states with the configuration  $6snl$  arises from separate contributions from the  $6s$  core and  $nl$  Rydberg electrons [30]. The core potential  $U_c(\vec{R}) = -(1/2\epsilon_0 c)\alpha_c(\omega)I(\vec{R})$  is derived from the dynamic electric dipole polarizability  $\alpha_c(\omega)$  of the  $\text{Yb}^+$  ion  $6s^2S_{1/2}$  state (here,  $I(\vec{R})$  is the light intensity at the nuclear coordinate  $\vec{R}$ ,  $\epsilon_0$  is the permittivity of free space, and  $c$  is the speed of light). For the 532 nm light used here, this is of the same order of magnitude as the  $\text{Yb}^0$  ground state potential, as the principal  $\text{Yb}^+$  transitions (369, 329 nm) are not too far from the principal  $\text{Yb}^0$  transition (399 nm). The nearly free Rydberg electron experiences a ponderomotive potential that depends on the intensity averaged over its wave function [19]:

$$U_r(\vec{R}) = \frac{e^2}{2\epsilon_0 c m_e \omega^2} \int |\psi_{nl}(\vec{r})|^2 I(\vec{r} + \vec{R}) d^3\vec{r}. \quad (1)$$

Here,  $\psi_{nl}(\vec{r})$  is the wave function of the  $nl$  electron ( $\vec{r}$  is the electron coordinate relative to the nucleus; Fig. 1(b)). In Fig. 1(c), the sum of these contributions for the  $^3S_1$  Rydberg states in an optical tweezer ( $\lambda = 532$  nm,  $1/e^2$  radius  $w_0 = 650$  nm) is shown as a function of the principal quantum number  $n$ . For low  $n$  where the Rydberg wave function is significantly smaller than the beam waist, the total polarizability is  $\alpha_c(\omega) - e^2/m\omega^2$ , while at high  $n$  it asymptotes to  $\alpha_c(\omega)$ , as the overlap of the Rydberg electron with the tweezer decreases.

We characterize the trapping potential for Yb Rydberg states using an array of six optical tweezers loaded with single  $^{174}\text{Yb}$  atoms, which are detected using fluorescence on the  $^3P_1$  transition with a fidelity greater than 99%, using the method and apparatus of Ref. [15]. A large array spacing ( $d = 24 \mu\text{m}$ ) minimizes the influence of interactions on the spectroscopy. We excite atoms to Rydberg states using sequential single-photon  $\pi$  pulses on the  $^1S_0 \rightarrow ^3P_1(M_J = -1)$  and  $^3P_1(M_J = -1) \rightarrow 6sns^3S_1(M_J = -1)$  transitions, as shown in Fig. 2(d). This configuration is somewhat inefficient because of the finite lifetime of the intermediate state (860 ns), but avoids noise on our 556 nm

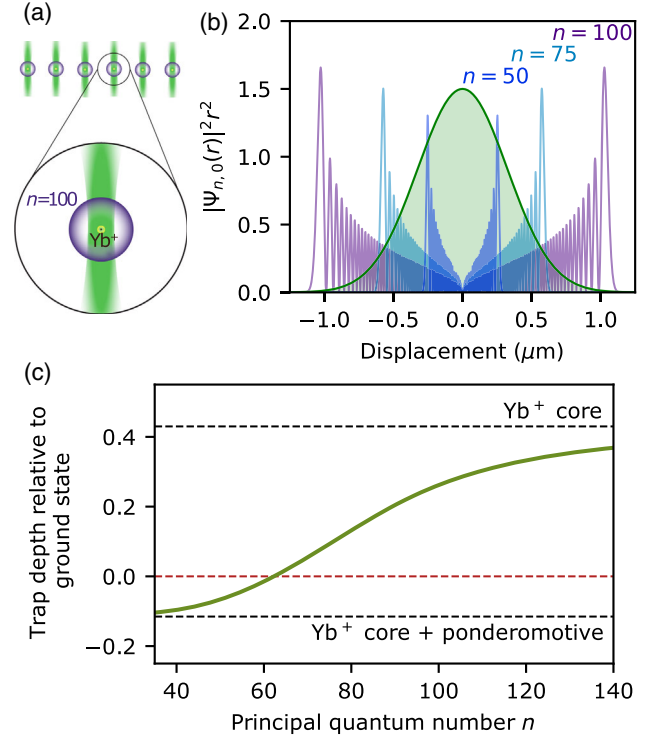


FIG. 1. (a) Cartoon of the experiment, showing a six-tweezer array, the Rydberg electron wave function, and the  $\text{Yb}^+$  ion core. (b) Radial probability distributions of Rydberg wave functions relative to the optical tweezers (green). (c) Calculated trap depth for  $^3S_1$  states, normalized to the trap depth for the  $^1S_0$  ground state for the same power and beam waist (here,  $0.65 \mu\text{m}$ ).

laser system that was not designed for coherent two-photon excitation. The absolute Rydberg excitation probability is about 0.4. The 308 nm light for the Rydberg transition is generated by summing a Ti:Sapphire laser with a 1565 nm fiber laser and doubling the 616 nm output in a resonant cavity. We have generated more than 100 mW in this configuration, but the experiments described here used approximately 5 mW focused to  $10 \mu\text{m}$ . We primarily study the Yb  $6sns^3S_1$  series, which has not been previously observed to the best of our knowledge. The series is relatively unperturbed, with a quantum defect of approximately 4.438 (additional details are provided in the Supplemental Material [31]). For this state, we achieve a Rabi frequency of  $\Omega = 2\pi \times 2.5$  MHz from  $^3P_1$ .

We measure the trapped lifetime of a Rydberg atom by imaging the ground state atoms, exciting to a particular Rydberg state, waiting a variable time  $\tau$ , and deexciting using a second UV laser pulse before acquiring a second image. If the Rydberg atom leaves the trap or changes states between the UV pulses (i.e., from spontaneous decay or interaction with blackbody radiation), it will not be deexcited by the second pulse and will be recorded as an atom loss between the two images. All data are averaged over six sites. A typical trace for the  $n = 75$   $^3S_1$  state is shown in Fig. 2(a) using 9 mW per trap (12 MHz ground

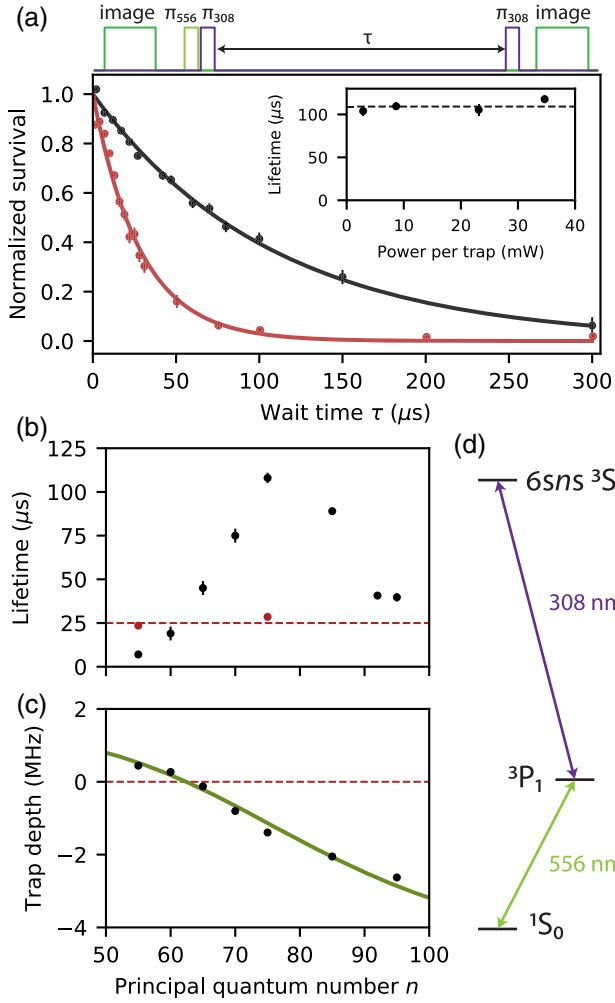


FIG. 2. (a) Survival probability of the  $n = 75$   $^3S_1$  state with (black,  $\tau = 108 \mu\text{s}$ ) and without (red,  $\tau = 28 \mu\text{s}$ ) the traps. Inset: Trapped Rydberg lifetime  $\tau$  of the  $^3S_1$  Rydberg state vs trap power at  $n = 75$ . (b) Trapped Rydberg lifetime of the  $^3S_1$  state vs principal quantum number  $n$ , with (black) and without (red) the trap. The dashed red line shows the untrapped lifetime of a ground state atom under the same conditions. (c) Trap depth of the  $^3S_1$  Rydberg state vs principal quantum number. The green line is the theoretical trap depth using the calculation from Fig. 1(c). (d) Relevant Yb energy levels for Rydberg excitation.

state trap depth). If the trap is turned off between the UV pulses, the Rydberg atom survives for  $28 \mu\text{s}$ , consistent with the measured ground state lifetime in the absence of a trap. When the trap is on between the UV pulses, the lifetime is extended to  $108 \mu\text{s}$ . To investigate the role of trap-induced loss processes such as photo- or autoionization of the Rydberg state, we measure the lifetime as a function of the trap depth, shown in the Fig. 2(a) inset. We observe no influence of the trap depth on the lifetime over a wide range of powers.

We repeat these measurements at several values of principal quantum number  $n$ . At low  $n$  (e.g.,  $n = 55$ ), the lifetime with the trap is shorter than without the trap,

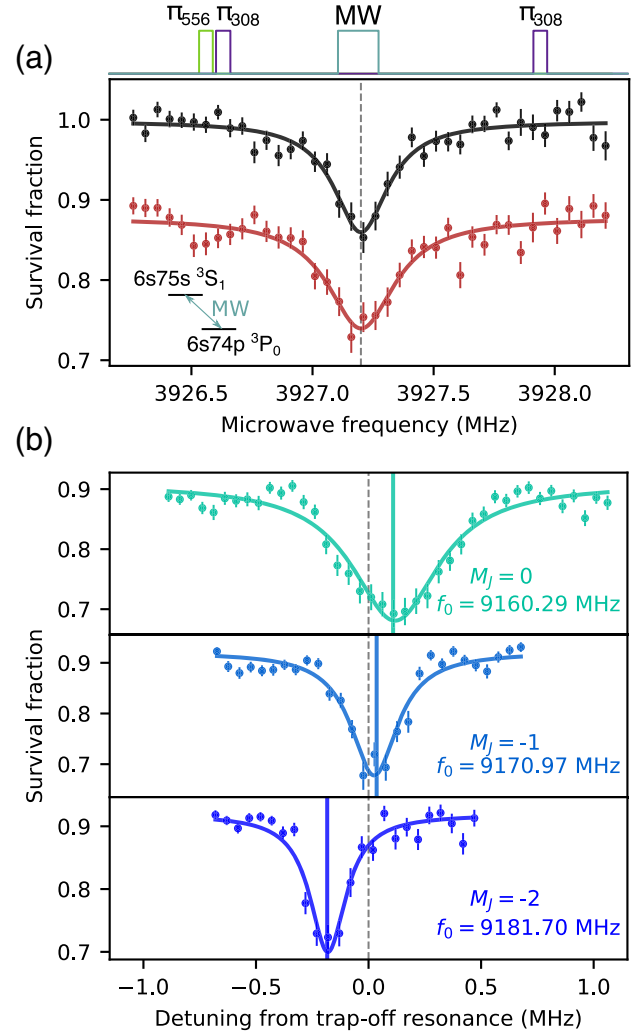


FIG. 3. (a) Microwave spectrum of the  $n = 75$   $^3S_1$  to  $n = 74$   $^3P_0$  transition with (black) and without (red) the traps, demonstrating the magic trapping condition. The black data are shifted for clarity and the solid lines are Lorentzian fits. (b) Microwave spectra of the  $n = 75$   $^3S_1$   $M_J = -1$  to  $n = 74$   $^3P_2$   $M_J = -2, -1, 0$  transitions, showing the tensor light shift of different  $M_J$  levels from the ponderomotive potential. For each transition, zero detuning indicates the measured transition frequency without the trap, indicated in the figure. The solid vertical lines show the predicted  $M_J^2$  dependence of the tensor light shift.

suggesting that these states are repelled. Above  $n \approx 60$ , the trapped lifetimes are longer, consistent with trapping. Curiously, they reach a maximum at  $n = 75$  and then decrease, although the intrinsic Rydberg lifetimes are expected to increase monotonically as  $n^2$ . We do not observe any trap power dependence of the lifetime between  $n = 70$  and  $n = 95$ , ruling out trap-induced losses. We conjecture that noise or cavity effects from our in-vacuum electrodes may play a role in the reduction of the lifetime [31].

To study the interplay of the ponderomotive and core ion polarizabilities, we measure the trap depth as a function of  $n$  using the ac stark shift of the UV  $^3P_1$  to  $^3S_1$  transition.

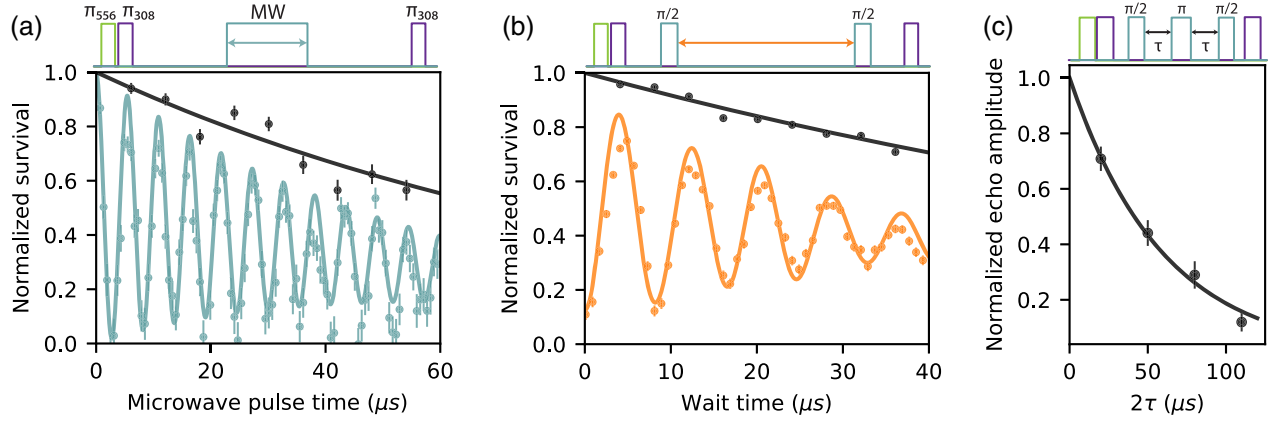


FIG. 4. (a) Two-photon Rabi oscillations between  $n = 75$   $^3S_1$  and  $n = 74$   $^3S_1$ . The solid line is a cosine fit with exponential decay time  $\tau = 42$   $\mu\text{s}$ . Control data without microwave pulses (black data) shows  $T_1$  for comparison. (b) Ramsey measurement of  $T_2^*$ . The orange line is a simulation that takes into account dephasing from the differential light shift between the two levels (90 kHz) and a finite atomic temperature (13  $\mu\text{K}$ ), yielding a  $1/e$  decay time of 22  $\mu\text{s}$ . (c) Hahn echo measurement. The black line is an exponential fit that yields  $T_2 = 59$   $\mu\text{s}$ .

We measure a crossover from antitrapping to trapping around  $n = 60$ , consistent with the onset of the lifetime increase. To obtain the absolute shift of the Rydberg state in the trap, we subtract the  $^3P_1$  trap depth, which we infer from the measured  $^3P_1$ - $^1S_0$  light shift in the trap (7.54 MHz) and the ratio of the polarizabilities of these states  $R = \alpha_{^3P_1}/\alpha_{^1S_0} \approx 0.39$  [55]. Because of uncertainty in  $R$ , there is a systematic uncertainty of  $\sim 0.2$  MHz in the Rydberg trap depth, which allows the crossover  $n$  between trapping and antitrapping to vary between 56 and 63. Fixing it at  $n = 62$  gives good agreement with a model with  $w_0 = 650$  nm and  $\alpha_c(532 \text{ nm}) = 107$  a.u., within 12% of the value calculated in Ref. [56].

Next we study the state-dependent nature of the trapping potential by driving microwave transitions between Rydberg states following optical excitation to a  $^3S_1$  state (Fig. 3). The shift of the microwave transition when the dipole trap is applied probes the differential polarizability of these states. The  $^3S_1$  and  $^3P_0$  states have nearly vanishing differential polarizability: on top of an estimated trap depth of 1.4 MHz, the transition frequency shifts less than 10 kHz. This is in agreement with a theoretical prediction [31] that the  $^1S_0$ ,  $^3S_1$ , and  $^3P_0$  states should experience the same, purely scalar, ponderomotive potential, and the fact that the ion core polarizability is independent of the state of the Rydberg electron. In contrast, the  $^3P_2$  state has a strong  $M_J$ -dependent shift arising from the rank-2 (tensor) component of the ponderomotive potential [Fig. 3(b)]. Intuitively, this results from the different orientations of the  $M_J$  angular wave functions with respect to the tweezer potential, which is not spherically symmetric. The observed tensor shift of 300 kHz is close to the computed value of 400 kHz using the model parameters discussed above.

We have also measured the lifetimes of several  $P$  and  $D$  states, presented in the Supplemental Material [31]. Near

$n = 75$ , the  $^3P_2$  and  $^1D_2$  lifetimes are similar to  $^3S_1$ , while the  $^3P_0$  lifetime is nearly 10 times shorter, presumably because this series is very strongly perturbed [57]. However, both  $P$  and  $D$  states experience a moderate reduction in lifetime with increasing trap power, attributable to photoionization. The approximate magnitude and  $L$  dependence are in approximate agreement with previous calculations for Rb [58].

To demonstrate the utility of trapping Rydberg states for quantum simulation and quantum computing, we probe the coherence properties of a superposition of Rydberg levels. In Fig. 4(a), we show Rabi oscillations between the  $n = 74$  and  $n = 75$   $^3S_1$  states, driven by a two-photon microwave transition detuned by 40 MHz from the  $^3P_0$  intermediate state. The oscillations persist for more than 60  $\mu\text{s}$ , more than twice the lifetime of an untrapped Rydberg atom. The coherence time is quantified using a Ramsey sequence [Fig. 4(b)] and found to be  $T_2^* = 22$   $\mu\text{s}$ , which is in agreement with dephasing from thermal motion [59] for an atom with a temperature of  $T = 13$   $\mu\text{K}$  and the (measured) difference in the potential depth for the two states of 90 kHz. A Hahn echo sequence yields  $T_2 = 59$   $\mu\text{s}$ . We note that this is shorter than the limit  $T_2 = T_1$  (here,  $T_1$  is the lifetime of the upper and lower states of the transition), which may arise in part from imperfect dynamical decoupling of the differential light shift arising from the axial trap motion, with an estimated period of 200  $\mu\text{s}$ .

These results demonstrate that trapping Rydberg states of alkaline earth atoms using the core polarizability can extend the coherence of quantum operations beyond what is possible with untrapped atoms. This will lead to improved fidelities for quantum simulators and Rydberg gates leveraging interactions between alkaline earth atom Rydberg states, as recently demonstrated in Sr [16]. The expected improvement from trapping Rydberg states is

most significant when the Rydberg lifetimes are very long, as expected for low- $l$  states at cryogenic temperatures, and especially circular Rydberg states.

We conclude with a discussion of several aspects of these results. First, the coherence times in Fig. 4 are limited by a slight  $n$  dependence of the trapping potential. While the ponderomotive potential itself is only weakly  $n$  dependent, the fractional  $n$  dependence is large when it is almost completely cancelled by the  $n$  independent core potential. A higher degree of state-insensitive trapping can be realized by using higher  $n$  states or by using shorter wavelength trapping light (to increase the relative contribution of the core polarizability) or smaller beam waist. Tuning the beam waist allows the precise potential for a particular Rydberg state to be manipulated, which may be advantageous for fine-tuning triply magic trapping of ground, clock, and Rydberg states [60].

Second, we consider the prospect of trapping circular Rydberg states of Yb, which have been predicted to have lifetimes of tens of seconds in cryogenic microwave cavities [21,22]. While photoionization shortens the lifetime of  $P$  and  $D$  states by 15–30%, the photo- and autoionization cross sections both decrease rapidly with  $L$  and are negligible for circular states [21], enabling long trapping times. Furthermore, transfer of orbital angular momentum from focused Laguerre-Gauss modes through the ponderomotive potential offers an intriguing new route to rapidly exciting circular Rydberg states [61] or driving transitions between them [22].

We gratefully acknowledge Tom Gallagher and Patrick Cheinet for helpful conversations about Yb Rydberg states, Shimon Kolkowitz for discussions about the manuscript, and Toptica Photonics for the loan of a WS8-2 wave meter used for the Rydberg spectroscopy. This work was supported by the Army Research Office (Contract No. W911NF-18-1-0215) and the Sloan Foundation. J. T. W. was supported by an NSF GRFP. S. S. was supported by an ARO QuaGCR fellowship. Y. M. was supported by the Austrian Science Fund (DK CoQuS Project No. W 1210-N16).

J. T. W. and S. S. contributed to this work equally.

\*Corresponding author.

jdthompson@princeton.edu

- [1] M. D. Lukin, M. Fleischhauer, R. Cote, L. M. Duan, D. Jaksch, J. I. Cirac, and P. Zoller, *Phys. Rev. Lett.* **87**, 037901 (2001).
- [2] M. Saffman, T. G. Walker, and K. Mølmer, *Rev. Mod. Phys.* **82**, 2313 (2010).
- [3] H. Bernien, S. Schwartz, A. Keesling, H. Levine, A. Omran, H. Pichler, S. Choi, A. S. Zibrov, M. Endres, M. Greiner, V. Vuletić, and M. D. Lukin, *Nature (London)* **551**, 579 (2017).
- [4] V. Lienhard, S. de Léséleuc, D. Barredo, T. Lahaye, A. Browaeys, M. Schuler, L. P. Henry, and A. M. Läuchli, *Phys. Rev. X* **8**, 021070 (2018).
- [5] S. de Léséleuc, V. Lienhard, P. Scholl, D. Barredo, S. Weber, N. Lang, H. P. Büchler, T. Lahaye, and A. Browaeys, *Science* **365**, 775 (2019).
- [6] E. Urban, T. A. Johnson, T. Henage, L. Isenhower, D. D. Yavuz, T. G. Walker, and M. Saffman, *Nat. Phys.* **5**, 110 (2009).
- [7] T. Wilk, A. Gaëtan, C. Evellin, J. Wolters, Y. Miroshnychenko, P. Grangier, and A. Browaeys, *Phys. Rev. Lett.* **104**, 010502 (2010).
- [8] Y. Y. Jau, A. M. Hankin, T. Keating, I. H. Deutsch, and G. W. Biedermann, *Nat. Phys.* **12**, 71 (2016).
- [9] H. Levine, A. Keesling, A. Omran, H. Bernien, S. Schwartz, A. S. Zibrov, M. Endres, M. Greiner, V. Vuletić, and M. D. Lukin, *Phys. Rev. Lett.* **121**, 123603 (2018).
- [10] H. Levine, A. Keesling, G. Semeghini, A. Omran, T. T. Wang, S. Ebadi, H. Bernien, M. Greiner, V. Vuletić, H. Pichler, and M. D. Lukin, *Phys. Rev. Lett.* **123**, 170503 (2019).
- [11] T. M. Graham, M. Kwon, B. Grinkemeyer, Z. Marra, X. Jiang, M. T. Lichtman, Y. Sun, M. Ebert, and M. Saffman, *Phys. Rev. Lett.* **123**, 230501 (2019).
- [12] A. Omran, H. Levine, A. Keesling, G. Semeghini, T. T. Wang, S. Ebadi, H. Bernien, A. S. Zibrov, H. Pichler, S. Choi, J. Cui, M. Rossignolo, P. Rembold, S. Montangero, T. Calarco, M. Endres, M. Greiner, V. Vuletić, and M. D. Lukin, *Science* **365**, 570 (2019).
- [13] A. Cooper, J. P. Covey, I. S. Madjarov, S. G. Porsev, M. S. Safronova, and M. Endres, *Phys. Rev. X* **8**, 041055 (2018).
- [14] M. A. Norcia, A. W. Young, and A. M. Kaufman, *Phys. Rev. X* **8**, 041054 (2018).
- [15] S. Saskin, J. T. Wilson, B. Grinkemeyer, and J. D. Thompson, *Phys. Rev. Lett.* **122**, 143002 (2019).
- [16] I. S. Madjarov, J. P. Covey, A. L. Shaw, J. Choi, A. Kale, A. Cooper, H. Pichler, V. Schkolnik, J. R. Williams, and M. Endres, *Nat. Phys.* **16**, 857 (2020).
- [17] M. A. Norcia, A. W. Young, W. J. Eckner, E. Oelker, J. Ye, and A. M. Kaufman, *Science* **366**, 93 (2019).
- [18] I. S. Madjarov, A. Cooper, A. L. Shaw, J. P. Covey, V. Schkolnik, T. H. Yoon, J. R. Williams, and M. Endres, *Phys. Rev. X* **9**, 041052 (2019).
- [19] S. K. Dutta, J. R. Guest, D. Feldbaum, A. Walz-Flannigan, and G. Raithel, *Phys. Rev. Lett.* **85**, 5551 (2000).
- [20] M. Archimi, C. Simonelli, L. Di Virgilio, A. Greco, M. Ceccanti, E. Arimondo, D. Ciampini, I. I. Ryabtsev, I. I. Beterov, and O. Morsch, *Phys. Rev. A* **100**, 030501(R) (2019).
- [21] T. L. Nguyen, J. M. Raimond, C. Sayrin, R. Cortiñas, T. Cantat-Moltrecht, F. Assemat, I. Dotsenko, S. Gleyzes, S. Haroche, G. Roux, T. Jolicœur, and M. Brune, *Phys. Rev. X* **8**, 011032 (2018).
- [22] S. R. Cohen and J. D. Thompson, *PRX Quantum* **2**, 030322 (2021).
- [23] D. Barredo, V. Lienhard, P. Scholl, S. de Léséleuc, T. Boulier, A. Browaeys, and T. Lahaye, *Phys. Rev. Lett.* **124**, 023201 (2020).
- [24] S. E. Anderson, K. C. Younge, and G. Raithel, *Phys. Rev. Lett.* **107**, 263001 (2011).

- [25] L. Li, Y. O. Dudin, and A. Kuzmich, *Nature (London)* **498**, 466 (2013).
- [26] D. A. Anderson, A. Schwarzkopf, R. E. Sapiro, and G. Raithel, *Phys. Rev. A* **88**, 031401(R) (2013).
- [27] S. D. Hogan and F. Merkt, *Phys. Rev. Lett.* **100**, 043001 (2008).
- [28] R. G. Cortiñas, M. Favier, B. Ravon, P. Méhaignerie, Y. Machu, J. M. Raimond, C. Sayrin, and M. Brune, *Phys. Rev. Lett.* **124**, 123201 (2020).
- [29] R. Mukherjee, J. Millen, R. Nath, M. P. A. Jones, and T. Pohl, *J. Phys. B* **44**, 184010 (2011).
- [30] T. Topcu and A. Derevianko, *Phys. Rev. A* **89**, 023411 (2014).
- [31] See Supplemental Material at <http://link.aps.org/supplemental/10.1103/PhysRevLett.128.033201>, which includes Refs. [32–54], for additional information about the trapping potential calculation, as well as supplementary experimental data and analysis.
- [32] K. Guo, G. Wang, and A. Ye, *J. Phys. B* **43**, 135004 (2010).
- [33] V. A. Dzuba and A. Derevianko, *J. Phys. B* **43**, 074011 (2010).
- [34] T. Topcu and A. Derevianko, *Phys. Rev. A* **88**, 043407 (2013).
- [35] B. Knuffman and G. Raithel, *Phys. Rev. A* **75**, 053401 (2007).
- [36] A. R. Edmonds, *Angular Momentum in Quantum Mechanics* (Princeton University Press, Princeton, NJ, 1996).
- [37] J. Neukammer, H. Rinneberg, and U. Majewski, *Phys. Rev. A* **30**, 1142 (1984).
- [38] A. E. Siegman, *Lasers* (University Science Books, Mill Valley, 1986).
- [39] L. Couturier, I. Nosske, F. Hu, C. Tan, C. Qiao, Y. H. Jiang, P. Chen, and M. Weidemüller, *Phys. Rev. A* **99**, 022503 (2019).
- [40] J. Hostetter, J. D. Pritchard, J. E. Lawler, and M. Saffman, *Phys. Rev. A* **91**, 012507 (2015).
- [41] L. Nenadovi and J. J. McFerran, *J. Phys. B* **49**, 065004 (2016).
- [42] K. Pandey, A. K. Singh, P. V. Kiran Kumar, M. V. Suryanarayana, and V. Natarajan, *Phys. Rev. A* **80**, 022518 (2009).
- [43] H. Lehec, A. Zuliani, W. Maineult, E. Luc-Koenig, P. Pillet, P. Cheinet, F. Niyaz, and T. F. Gallagher, *Phys. Rev. A* **98**, 062506 (2018).
- [44] S. Weber, C. Tresp, H. Menke, A. Urvoy, O. Firstenberg, H. P. Büchler, and S. Hofferberth, *J. Phys. B* **50**, 133001 (2017).
- [45] C. L. Vaillant, M. P. Jones, and R. M. Potvliege, *J. Phys. B* **45**, 135004 (2012).
- [46] S. Olmschenk, D. Hayes, D. N. Matsukevich, P. Maunz, D. L. Moehring, K. C. Younge, and C. Monroe, *Phys. Rev. A* **80**, 022502 (2009).
- [47] W. E. Cooke, T. F. Gallagher, S. A. Edelstein, and R. M. Hill, *Phys. Rev. Lett.* **40**, 178 (1978).
- [48] E. Y. Xu, Y. Zhu, O. C. Mullins, and T. F. Gallagher, *Phys. Rev. A* **33**, 2401 (1986).
- [49] C. B. Xu, X. Y. Xu, W. Huang, M. Xue, and D. Y. Chen, *J. Phys. B* **27**, 3905 (1994).
- [50] G. Fields, X. Zhang, F. B. Dunning, S. Yoshida, and J. Burgdörfer, *Phys. Rev. A* **97**, 013429 (2018).
- [51] W. E. Cooke and T. F. Gallagher, *Phys. Rev. A* **19**, 2151 (1979).
- [52] T. F. Gallagher, *Rydberg Atoms* (Cambridge University Press, Cambridge, 1994).
- [53] A. Burgess and M. J. Seaton, *Rev. Mod. Phys.* **30**, 992 (1958).
- [54] C. L. Vaillant, M. P. A. Jones, and R. M. Potvliege, *J. Phys. B* **47**, 155001 (2014).
- [55] R. Yamamoto, J. Kobayashi, T. Kuno, K. Kato, and Y. Takahashi, *New J. Phys.* **18**, 023016 (2016).
- [56] A. Roy, S. De, B. Arora, and B. K. Sahoo, *J. Phys. B* **50**, 205201 (2017).
- [57] M. Aymar, R. J. Champeau, C. Delsart, and O. Robaux, *J. Phys. B* **17**, 3645 (1984).
- [58] M. Saffman and T. G. Walker, *Phys. Rev. A* **72**, 022347 (2005).
- [59] S. Kuhr, W. Alt, D. Schrader, I. Dotsenko, Y. Miroshnichenko, A. Rauschenbeutel, and D. Meschede, *Phys. Rev. A* **72**, 023406 (2005).
- [60] T. Topcu and A. Derevianko, *J. Phys. B* **49**, 144004 (2016).
- [61] R. Cardman and G. Raithel, *Phys. Rev. A* **101**, 013434 (2020).